Proc. Natl. Acad. Sci. USA
Vol. 96, pp. 3664–3669, March 1999
Biophysics

Spin-lattice relaxation of laser-polarized xenon in human blood

JAN WOLBER*, ANDREA CHERUBINI*†, ANDRZEJ S. K. DZIK-JURASZ*, MARTIN O. LEACH*, AND ANGELO BIFONE*‡

*Cancer Research Campaign Clinical Magnetic Resonance Research Group, The Institute of Cancer Research, The Royal Marsden National Health Service Trust, Sutton, Surrey SM2 5PT, United Kingdom; and †Department of Physics, University of Rome "La Sapienza," P.le Aldo Moro 2, 000185 Rome, Italy

Communicated by Alexander Pines, University of California, Berkeley, CA, January 25, 1999 (received for review November 18, 1998)

ABSTRACT **The nuclear spin polarization of ^{129}Xe can be enhanced by several orders of magnitude by using optical pumping techniques. The increased sensitivity of xenon NMR has allowed imaging of lungs as well as other *in vivo* applications. The most critical parameter for efficient delivery of laser-polarized xenon to blood and tissues is the spin-lattice relaxation time (T_1) of xenon in blood. In this work, the relaxation of laser-polarized xenon in human blood is measured *in vitro* as a function of blood oxygenation. Interactions with dissolved oxygen and with deoxyhemoglobin are found to contribute to the spin-lattice relaxation time of ^{129}Xe in blood, the latter interaction having greater effect. Consequently, relaxation times of ^{129}Xe in deoxygenated blood are shorter than in oxygenated blood. In samples with oxygenation equivalent to arterial and venous blood, the ^{129}Xe T_1s at 37°C and a magnetic field of 1.5 T were 6.4 s ± 0.5 s and 4.0 s ± 0.4 s, respectively. The ^{129}Xe spin-lattice relaxation time in blood decreases at lower temperatures, but the ratio of T_1 in oxygenated blood to that in deoxygenated blood is the same at 37°C and 25°C. A competing ligand has been used to show that xenon binding to albumin contributes to the ^{129}Xe spin-lattice relaxation in blood plasma. This technique is promising for the study of xenon interactions with macromolecules.**

Optical pumping of rubidium vapor with circularly polarized laser light and spin exchange with ^{129}Xe or ^{3}He nuclei enhances the nuclear spin polarization by several orders of magnitude (1, 2) and allows NMR detection of xenon or helium in very low concentration (3). The laser-polarized gas, often referred to as hyperpolarized gas, can be imaged directly in the airways of the lungs after introduction into the respiratory system. This technique has been applied successfully in lung ventilation studies (4, 5). Furthermore, the high solubility of xenon in blood and lipids and the wide range of chemical shifts of xenon in different solvents (6) suggests a variety of *in vivo* MR applications, including functional imaging, investigation of blood flow, and studies of perfusion, blood volume, and permeability.

One of the major challenges for MR applications of hyperpolarized xenon is the efficient delivery of gas to blood and organs of interest while maintaining a large nonequilibrium polarization. The simplest administration route is via the respiratory system. Preliminary ^{129}Xe MR images of xenon in brain have been obtained with this technique in an animal model (7). Compartmental models have been used to predict the concentration of hyperpolarized xenon in human tissues (8, 9) after administration to the lungs. Many parameters that determine xenon dynamics in lungs, circulatory system, and tissues have been well characterized in radioactive nuclear imaging studies (for a review see ref. 9). In contrast, some critical NMR parameters, such as ^{129}Xe relaxation times in blood, lungs, and tissues, are still under investigation. The spin-lattice relaxation time (T_1) for xenon mixed with oxygen in the lungs (typically 80% xenon and 20% oxygen) is in the range of 10–30 s (10, 11). The spin-lattice relaxation time of ^{129}Xe in blood determines the loss of polarization during transit from the lungs to the tissue of interest. Therefore, the signal from xenon in tissue depends critically on ^{129}Xe T_1 in the blood (9). A difference in the relaxation times of xenon in oxygenated and deoxygenated blood could be used as a contrast mechanism in functional MRI, where blood would act as an endogenous contrast agent. The ^{129}Xe spin-lattice relaxation time in blood and its dependence on the blood oxygenation level, however, are still matter of contention (12–16).

Albert *et al.* (12) measured the ^{129}Xe spin-lattice relaxation time in blood at 2.35 T by using thermally polarized xenon. Values of 4.5 s and 9.6 s for xenon dissolved in the red blood cells and in plasma were reported. The blood oxygenation level in these experiments was approximately 20%. The long measurement times (12) caused the blood samples to separate out, which may explain the different relaxation times found in the two compartments. Experiments performed by Bifone *et al.* (13) with hyperpolarized xenon have shown that the rapid exchange time between red blood cells and plasma (12 ms) yields a single T_1 for ^{129}Xe in both compartments. Those authors report a T_1 of 5 s at a field of 9.4 T. In these experiments, the hyperpolarized gas was introduced by injecting a small amount of saline equilibrated with xenon into the blood sample in an open tube placed in the NMR coil. Exchange of gas at the sample surface might have affected the relaxation time measurement. No attempt was made to measure the dependence of the relaxation time on the oxygenation state of the blood.

Albert *et al.* (14) performed experiments at a field strength of 1.5 T showing a dependence of the xenon relaxation time on blood oxygenation. Those authors found a significantly longer ^{129}Xe T_1 in oxygenated blood. This result indicates interaction with paramagnetic deoxyhemoglobin (17, 18) as the dominant relaxation mechanism for ^{129}Xe in blood. In these experiments, the hyperpolarized gas was introduced by bubbling xenon into blood samples that had been substantially diluted with saline. Albert *et al*. report that a strong signal from gaseous ^{129}Xe could be detected, suggesting that gas exchange may have perturbed the relaxation time measurement. Because of the dilution of the samples, only the signal of xenon in saline and plasma could be detected, whereas the signal from xenon in the blood cells dropped below the level of noise. Therefore, the relaxation times had to be determined solely from the decay of the saline/plasma signal, and relaxation times in oxygenated and deoxygenated blood were extrapolated from measurements at different dilutions. Furthermore, gas exchange from bubbling xenon through the sample might have altered the blood oxygenation level during the experiment.

Tseng *et al.* (15) measured T_1 of hyperpolarized ^{129}Xe in blood foam at 4.7 T. These experiments have shown the opposite dependence of the xenon relaxation time on blood oxygenation compared with ref. 14. Values of 21 s and over 40 s

The publication costs of this article were defrayed in part by page charge payment. This article must therefore be hereby marked "*advertisement*" in accordance with 18 U.S.C. §1734 solely to indicate this fact.

PNAS is available online at www.pnas.org.

‡To whom reprint requests should be addressed. e-mail: bifone@icr.ac.uk.

were reported for oxygenated and deoxygenated blood, implying that interaction with paramagnetic oxygen in solution is the main cause of ^{129}Xe relaxation. The foam presents a large exchange surface between the gas compartment and the blood. Oxygen, as well as xenon, exchanges very efficiently with the dissolved phase, and the contribution of oxygen on the ^{129}Xe spin-lattice relaxation time may have been overestimated.

In this paper we present measurements of the spin-lattice relaxation time of hyperpolarized ^{129}Xe in human blood at a clinically relevant field of 1.5 T. Xenon dissolved in a small amount of saline was injected in a closed system containing blood equilibrated with different mixtures of gases. To ensure that the hematocrit was similar to typical *in vivo* values, a small amount of plasma was removed from the blood samples. After the injection, the sample tube was filled completely. No signal from gaseous xenon was observed in our experiments, which confirms that we have successfully prevented xenon exchange with the gas phase. We have determined the contribution of dissolved oxygen to the ^{129}Xe spin-lattice relaxation time by comparison of blood samples equilibrated with carbon monoxide and pure oxygen. The effect of paramagnetic deoxyhemoglobin was investigated by comparing samples equilibrated with different mixtures of oxygen and nitrogen. We found a temperature dependence of the relaxation times from measurements at 37°C and 25°C. We also have studied the xenon relaxation time in plasma and its dependence on dissolved oxygen and on the presence of ligands that bind to albumin.

MATERIALS AND METHODS

Optical Pumping. Optical pumping was performed by using equipment built in-house. Cylindrical glass cells of 60 cm^3 containing a visible amount of rubidium metal were filled with a mixture of 180 torr of isotopically enriched xenon (82% ^{129}Xe; Urenco, Almelo, The Netherlands) and 100 torr N_2 (BOC, Redhill, U.K.) and pressurized with approximately 10 bar of helium (BOC). The cell was placed in the 130 Gauss field of a Helmholtz magnet and heated to 125°C. Hyperpolarization was achieved by optical pumping of the D1 electron transition of the Rb vapor with circularly polarized light from a 90-W diode laser array (Opto Power, Tucson, AZ) and spin exchange to the ^{129}Xe nuclei. After 10–15 min of optical pumping, the cell was cooled to 80°C, and the xenon was collected in a distillator immersed in liquid nitrogen. During transport to the MR magnet, the frozen xenon was placed near one pole of a small horseshoe magnet to prevent rapid relaxation in zero magnetic field. The xenon was brought back to the gas phase in the bore of the MR magnet and admitted to the degassed saline, following the procedure described in detail in ref. 13. The gas was dissolved by vigorous shaking. The saline then was extracted, by using syringe and needle, through a self-sealing rubber septum, and injected into the blood sample in the NMR coil (see Fig. 1). The resulting ^{129}Xe gas polarization was typically between 5% and 10% in the MR magnet after freezing, transport, and thawing.

NMR Spectroscopy. All NMR experiments were performed by using a Siemens (Erlangen, Germany) Magnetom Vision 1.5 T clinical MR system. A home-built solenoid (^{129}Xe)/saddle (^{1}H/^{19}F) double-resonance coil was used. ^{129}Xe chemical shifts are expressed relative to gaseous ^{129}Xe (0 ppm).

For measuring ^{129}Xe, T_1, a variable flip angle NMR sequence was used. As the large nonequilibrium polarization is nonrenewable, each rf pulse irreversibly destroys a fraction of the magnetization. By increasing the flip angles of multipulse sequences, this loss can be compensated for, and no correction to the data is necessary to calculate the signal decay induced by T_1 processes (19, 20). We used a sequence of eight pulses with an inter-pulse delay of 1 s for measuring ^{129}Xe T_1 in blood and sequences of 12 pulses with inter-pulse delays between 1 and 4 s for the measurements in plasma and the protein

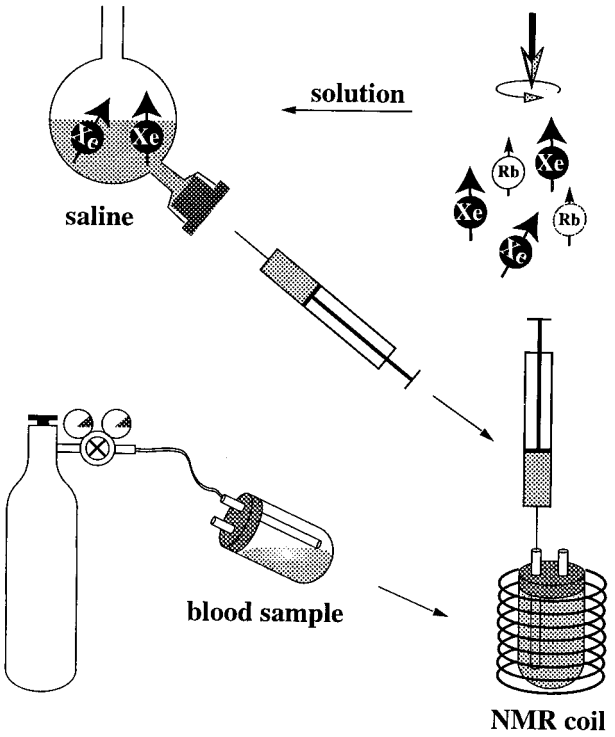

FIG. 1. Schematics of sample preparation: blood samples are equilibrated with gas from a cylinder, then the sample tube is placed in the NMR coil. Hyperpolarized xenon is dissolved in saline in custom-made glassware. A known amount of saline then is drawn into a syringe and injected into the blood sample, thereby filling the tube completely.

solutions. The flip angles θ_n were calculated according to $(sin^2\theta_{N-n})^{-1} = N - n + 1$, with N being the total number of pulses applied (see ref. 20). Rectangular pulses of 50 μs were used throughout, and the pulse amplitudes were varied to achieve the different flip angles.

Sample Preparation. Freshly drawn blood was left for about 1 hr in heparinized sample tubes at 4°C for the red blood cells to settle. Subsequently, part of the plasma was removed. To achieve different oxygenation levels, the samples were equilibrated with different gases in sample tubes sealed with a rubber septum with two thin glass capillaries for administering the gas (see Fig. 1). Gas was flushed through the tube for approximately 30 min. The sample was shaken gently to increase gas exchange while flushing. Vigorous bubbling of gas through the blood was avoided to prevent formation of highly paramagnetic methemoglobin, as methemoglobin can severely affect relaxation time measurements (the ^{129}Xe T_1 in metmyoglobin solution, for instance, has been reported to be as short as 5.2 ms in ref. 21). The content of methemoglobin was measured by spectrophotometry after the treatment, and its concentration was below the detection level. Immediately after the flushing procedure, the capillaries were closed to prevent gas exchange with air, and the sample was placed in the NMR coil. For the spin-lattice relaxation measurements, 1–1.5 ml of saline, equilibrated with one atmosphere of hyperpolarized xenon, was injected through one of the capillaries into the sample tube containing 3.6–4 ml of blood, filling the sample tube completely. No residual gas pockets were observed, nor was any signal detected from gaseous xenon. As part of the plasma had been removed, the hematocrit values of the samples were comparable to those of undiluted blood (see Table 1). Most importantly, introduction of the laser-polarized xenon in solution ensures that no macroscopic xenon gas compartment is present, and the xenon relaxation time is

Table 1. Summary of all sample parameters obtained from blood gas meter measurements

Sample	1	2	3	4	5	6	7
Gas	O_2	CO	N_2	Air	N_2	Mix*	Air
Temp (°C)	25	25	25	25	37	37	37
Hematocrit (%)	38	36	39	38	38	45	34
pH	7.66	7.58	7.94	7.63	7.72	7.41	7.43
pH corr.**	7.86	7.77	7.94	7.63	7.72	7.41	7.43
pCO_2 (kPa)	1.48	1.94	1.05	3.07	1.15	4.45	3.06
pCO_2 corr.** (kPa)	0.83	1.09	0.59	1.72	1.15	4.45	3.06
pO_2 (kPa)	71.0	–	1.95	5.88	3.15	6.84	10.84
pO_2 corr.** (kPa)	70.7	–	0.95	5.06	3.15	6.84	10.84
sO_2 (%)	100	–	39.8	83.1	67.2	86.2	96.3
sO_2 (%) corr.**	100	–	64.4	98.1	67.2	86.2	96.3

*, mixture of 90% N_2, 5% O_2, and 5% CO_2. **, blood gas analysis was performed at a sample temperature of 37°C throughout, whereas NMR measurements were performed at 25°C for samples 1–4. The corrections of pH, pCO_2, pO_2, and sO_2 for these samples were calculated by using standard hemoglobin saturation curves versus temperature to obtain the corresponding values at 25°C (*Materials and Methods*).

measured in a closed system. The sample preparation procedure is shown schematically in Fig. 1.

Immediately after the NMR experiments, the oxygenation level, sO_2, and the partial pressures of oxygen, pO_2, and carbon dioxide, pCO_2, were measured by using a blood gas analysis instrument (ABL 505, Radiometer, Copenhagen). These values are measured at a sample temperature of 37°C. Therefore, for samples measured at 25°C the values for pO_2, pCO_2, and sO_2 had to be corrected. This correction was done by using a numerical method accounting for the shift of the standard oxygen dissociation curve in blood with a 50% blood oxygenation level at a partial oxygen pressure of 3.578 kPa at 37°C (see ABL 505 manual, chapter 3, and refs. 22 and 23 cited therein).

The plasma samples were prepared by centrifuging freshly drawn blood at a temperature of 4°C at 2,000 rpm for 10 min. Subsequently, the plasma was frozen at −18°C. We performed two sets of experiments: for three samples we used the same preparation method as for the blood samples by equilibrating them with different gases and injecting a small amount of saline containing hyperpolarized xenon. One of these samples contained flucloxacillin sodium British Pharmacopia (BP) (Floxapen; Beecham Research, Hertfordshire, U.K.) in 100 mM concentration, which was chosen to investigate the effect of ligand binding to albumin on the xenon spin-lattice relaxation time in plasma. Two plasma samples, one with and one without flucloxacillin, were prepared in custom-made glassware in which the hyperpolarized xenon could be admitted directly to the plasma, and the gas was dissolved by shaking. We performed these measurements to investigate the effect of the small amount of saline on the ^{129}Xe relaxation time. Before introduction of the hyperpolarized gas, oxygen was removed from these samples by equilibrating the sample (1.5 ml) with 100 ml of helium for 20 min repeatedly. The same glassware and degassing procedure were used for measurements in albumin solution, which we performed to confirm whether flucloxacillin affects xenon binding to albumin. We used BSA powder (Sigma) and deuterated water with low paramagnetic impurity content (Aldrich). Flucloxacillin sodium BP was added in various concentrations to BSA/D_2O samples of 3 ml each.

RESULTS AND DISCUSSION

Blood samples with different oxygenation state were prepared as outlined in *Materials and Methods*. Oxygenation parameters for the blood samples are shown in Table 1. In addition to varying the oxygenation state of the blood and thereby changing the ratio of oxy- and deoxyhemoglobin, we investigated blood that was equilibrated with carbon monoxide (CO). The ^{125}Xe spin-lattice relaxation times for all samples are summarized in Table 2.

A typical hyperpolarized ^{129}Xe NMR spectrum of xenon in blood is shown in Fig. 2. The signal at a chemical shift of 197 ppm is caused by xenon in the saline/plasma mixture, whereas the signal at a chemical shift of 220 ppm corresponds to xenon in the red blood cells. The spectrum in Fig. 2 was obtained after a 21° rf pulse. The position of the signal of xenon in the red blood cells is shifted by 2–3 ppm downfield in samples equilibrated with pure oxygen and with CO, whereas the position of the saline/plasma signal is only shifted by a fraction of a ppm. The shift of the signal corresponding to xenon in the red blood cells may reflect the different susceptibilities in red blood cells containing oxygenated and deoxygenated hemoglobin, respectively.

The two peaks corresponding to xenon in the red blood cells and to xenon in plasma/saline were integrated to calculate the ^{129}Xe spin-lattice relaxation times in both environments. Because of the fast exchange of xenon between plasma and red blood cells (13), these two longitudinal relaxation times are identical within the experimental errors.

The contributions of dissolved oxygen and paramagnetic hemoglobin to the ^{129}Xe longitudinal relaxation time can be discriminated by comparing the measurements from different samples.

CO binds much more strongly than oxygen to hemoglobin, and full saturation with CO is achieved when equilibrating a blood sample with carbon monoxide. No effect on ^{129}Xe relaxation is expected from deoxyhemoglobin in either sample

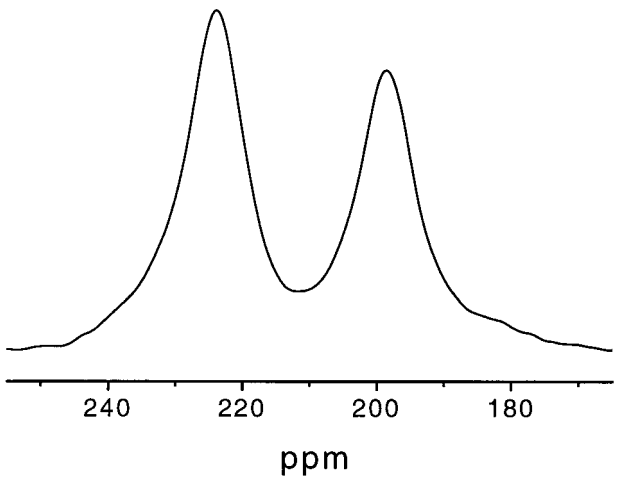

FIG. 2. Typical single-shot hyperpolarized ^{129}Xe NMR spectrum of xenon in blood. The flip angle applied was 21°. The signal at a chemical shift of 197 ppm is caused by xenon in the saline/plasma mixture, whereas the signal at a chemical shift of 222 ppm corresponds to xenon in the red blood cells.

Table 2. Hyperpolarized ^{129}Xe spin-lattice relaxation times for all blood samples

Sample	1	2	3	4	5	6	7
Gas	O_2	CO	N_2	Air	N_2	Mix*	Air
Temp (°C)	25	25	25	25	37	37	37
$T_{1,rbc}$ (*s*)	6.01 ± 0.26	7.72 ± 0.38	2.95 ± 0.24	5.11 ± 0.66	3.85 ± 0.15	4.00 ± 0.32	6.27 ± 0.33
$T_{1,plasma}(s)$	5.40 ± 0.27	7.97 ± 0.32	2.81 ± 0.16	5.26 ± 0.70	3.57 ± 0.18	3.90 ± 0.28	6.58 ± 0.42
$T_{1,average}(s)$	5.71 ± 0.35	7.84 ± 0.47	2.88 ± 0.27	5.19 ± 0.91	3.71 ± 0.22	3.95 ± 0.40	6.42 ± 0.50

The decay of the signal from xenon in plasma/saline and from xenon in the red blood cells were determined independently for both peaks. *, mixture of 90% N_2, 5% O_2, and 5% CO_2.

1, which is equilibrated with pure O_2, or in sample 2, which is equilibrated with CO. As shown in Table 1, full saturation of hemoglobin with oxygen is achieved in sample 1. In addition, this sample contains 70.7 kPa of dissolved oxygen. Therefore, the difference in longitudinal ^{129}Xe relaxation times for samples 1 and 2 should directly reflect the contribution of oxygen in solution. The ^{129}Xe T_1 is reduced from 7.84 s ± 0.47 s, in the sample equilibrated with CO, to 5.71 s ± 0.35 s, in the sample equilibrated with pure oxygen. The amount of dissolved oxygen in sample 1, however, is much larger than typical values for arterial blood (10–15 kPa). For the small difference in dissolved oxygen between arterial and venous blood, which is of the order of 5 kPa, this contribution to the ^{129}Xe T_1 in blood is smaller than that of deoxyhemoglobin, as discussed below.

Samples 5, 6, and 7 are equilibrated with pure N_2, with a mixture of 90% N_2, 5% O_2, and 5% CO_2, and with air, respectively. They provide information about the contribution of deoxyhemoglobin to the ^{129}Xe relaxation time. We have measured shorter ^{129}Xe T_1 for samples with higher concentrations of deoxyhemoglobin. In sample 7, hemoglobin is oxygenated to 96.3%, and the ^{129}Xe T_1 is 6.42 ± 0.50 s, compared with only 3.71 s ± 0.22 s in sample 5 with 67.2% hemoglobin oxygenation. We conclude that relaxation caused by deoxyhemoglobin is a very significant relaxation mechanism.

The same trend is observed when comparing samples 1, 3, and 4. Although sample 1 contains 70.7 kPa of dissolved oxygen (as opposed to only 0.95 kPa oxygen in sample 3), the corresponding ^{129}Xe T_1 of 5.71 s ± 0.35 s is almost twice as long as the ^{129}Xe relaxation time in sample 3, 2.88 s ± 0.27 s, which contains 64.4% oxyhemoglobin.

Decreasing the oxygenation of blood reduces the concentration of dissolved paramagnetic oxygen and increases the concentration of deoxyhemoglobin. The two relaxation mechanisms partially compensate each other. However, comparison of the results for samples 1, 3, and 4 shows that interaction of xenon with deoxyhemoglobin is by far the more efficient mechanism. In this context, the hematocrit of the sample is very important, as the contribution of deoxyhemoglobin depends strongly on concentration (14). The hematocrit values of our samples are all within the range of typical *in vivo* values (Table 1).

Both oxy- and carboxyhemoglobin are paramagnetic, whereas deoxyhemoglobin is paramagnetic (17). Xenon binding sites in horse hemoglobin have been identified by x-ray crystallography. These results indicate that the xenon binding sites on hemoglobin are located close to the G-H and A-B helix corner regions, respectively (24). Interaction with the paramagnetic metal ion is likely to be responsible for relaxation of ^{129}Xe in deoxyhemoglobin. Moreover, configurational changes induced by oxygen and carbon monoxide also could affect xenon binding to hemoglobin and contribute to the different relaxivities of oxy-, carboxy-, and deoxyhemoglobin.

Results for samples measured at temperatures of 37°C and 25°C show temperature dependence of the ^{129}Xe spin-lattice relaxation times. We observe shorter ^{129}Xe T_1s at lower temperature: the ^{129}Xe T_1 drops from 3.71 s ± 0.22 s at 37°C to 2.88 s ± 0.27 s at 25°C for the samples equilibrated with nitrogen (samples 5 and 3), and from 6.42 s ± 0.50 s at 37°C to 5.19 s ± 0.91 s at 25°C for the samples equilibrated with air (samples 7 and 4). The ratio of the relaxation times of oxygenated blood to those of deoxygenated blood, however, is the same at both temperatures within our experimental error.

From our results, we conclude that the ^{129}Xe T_1 in venous blood is shorter than that in arterial blood. As discussed, interaction with paramagnetic deoxyhemoglobin is more efficient than interaction with dissolved oxygen and determines the dependence of the xenon spin-lattice relaxation time on the oxygen saturation level. Samples 6 and 7 were measured at 37°C, and the blood oxygenation levels in these samples are very similar to physiological values (Table 1). Longitudinal ^{129}Xe relaxation times are 6.42 s ± 0.50 s for arterial blood and 3.95 s ± 0.40 s for venous blood.

The ^{129}Xe longitudinal relaxation time in plasma is longer than in full blood. We found a ^{129}Xe T_1 of 13.18 s ± 0.12 s in plasma equilibrated with air (sample P1). We also measured the longitudinal relaxation times of xenon in two plasma samples that were equilibrated with nitrogen. One of them contained 100 mM flucloxacillin. The results are summarized in Table 3. ^{129}Xe T_1 increases to 14.34 s ± 0.10 s when dissolved oxygen is removed (sample P2), and even further to 15.44 s ± 0.27 s upon introduction of flucloxacillin (sample P3). In samples P4 and P5, hyperpolarized xenon was introduced directly without using saline (as explained in *Materials and Methods*). The ^{129}Xe T_1 increases from 13.32 s ± 0.10 s in sample P4 to 16.17 s ± 0.19 s in sample P5, which contains flucloxacillin in 100 mM concentration. The position of the ^{129}Xe signal was shifted by 1 ppm downfield in the samples that contained flucloxacillin, compared with the samples without flucloxacillin.

From comparison of samples P4 and P5 with samples P2 and P3, we conclude that the introduction of a small amount of saline increases the xenon relaxation time by less than 10%. As the ^{129}Xe T_1 in full blood is determined mainly by mechanisms that are intracellular in origin, and as the hematocrit of our samples is comparable to *in vivo* conditions, our method of introducing the hyperpolarized xenon in solution into the blood represents only a very small perturbation. We notice, however, that the increase of the xenon spin-lattice relaxation time upon adding flucloxacillin is more pronounced in pure plasma (as can be seen from comparison of samples P4 and P5) than in the case of plasma that contains saline (samples P2 and

Table 3. Hyperpolarized ^{129}Xe spin-lattice relaxation times in all plasma samples

Sample	Preparation	T_1 (s)
P1	Equilibrated with air	13.18 ± 0.12
P2	Equilibrated with N_2	14.34 ± 0.10
P3	100 mM flucloxacillin, equilibrated with N_2	15.44 ± 0.27
P4	Equilibrated with He	13.32 ± 0.10
P5	100 mM flucloxacillin, equilibrated with He	16.17 ± 0.19

Samples P1–P3 were measured by adding a small amount of saline equilibrated with hyperpolarized xenon, whereas samples P4 and P5 were measured after admitting gaseous hyperpolarized xenon to the plasma.

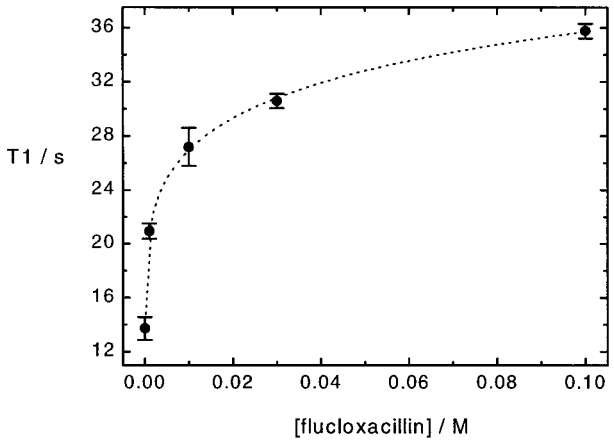

FIG. 3. Hyperpolarized ^{129}Xe T_1 in 5% (wt/vol) BSA in D_2O and different concentrations of flucloxacillin. Dotted line is a guide for the eye.

P3, respectively). The fact that the xenon relaxation time increases in the presence of flucloxacillin suggests that flucloxacillin acts as a competing ligand that is able to prevent xenon from binding to proteins in plasma. To verify this hypothesis, we performed experiments in 5% (wt/vol) BSA solution.

Plasma contains approximately 5% (wt/vol) albumin (see, for instance, ref. 25). To assess the contribution of protein binding to xenon relaxation in plasma, we conducted a series of measurements in a solution of 5% (wt/vol) BSA in fully deuterated water (D_2O) and various concentrations of flucloxacillin up to 100 mM. By using a fully deuterated solvent, we excluded cross-relaxation from xenon to water protons. Flucloxacillin, a fluorinated drug, displaces 5-fluorouracil from BSA, as shown from ^{19}F NMR spin-lattice relaxation time measurements (A.S.K. Dzik-Jurasz, personal communication; the use of ^{19}F NMR as a tool for studying ligand binding to macromolecules is reviewed in ref. 26). We measured hyperpolarized ^{129}Xe spin-lattice relaxation times in samples of different flucloxacillin concentration. Our results are displayed in Fig. 3. The xenon relaxation time is increased from 13.71 s $\pm$ 0.84 s in the pure 5% (wt/vol) BSA in D_2O solution to 35.77 s $\pm$ 0.55 s in 5% (wt/vol) BSA in D_2O and 100 mM flucloxacillin. The position of the ^{129}Xe signal was shifted by 2 ppm downfield in the sample containing 100 mM concentration of flucloxacillin compared with the 5% (wt/vol) BSA in D_2O solution sample.

Control experiments on a 100 mM flucloxacillin/D_2O solution and on pure D_2O show that xenon association with flucloxacillin does not significantly contribute to ^{129}Xe T_1. The dependence of solution viscosity on flucloxacillin concentration was measured by capillary viscometry. No significant effects were observed for flucloxacillin concentrations up to 100 mM. These findings suggest that xenon and flucloxacillin compete for one or more binding sites on BSA and that the presence of flucloxacillin affects xenon binding to the protein. Therefore, dipolar interaction between xenon and protons of the protein is reduced, which results in the longer spin-lattice relaxation time. Thus, we conclude that binding to albumin contributes to the longitudinal xenon relaxation time in plasma. However, as seen from comparison of samples P4 and P5, introduction of flucloxacillin changes the ^{129}Xe T_1 by only about 20%, and removal of dissolved oxygen changes the xenon relaxation time in plasma by less than 10%. This result indicates that other mechanisms, such as interaction with paramagnetic ions and other proteins (25), and cross-relaxation to the solvent contribute to xenon relaxation in plasma.

CONCLUSIONS

We have investigated the ^{129}Xe nuclear magnetic spin-lattice relaxation time in human blood *in vitro.* We have shown that interactions with dissolved oxygen and with paramagnetic deoxyhemoglobin both contribute to ^{129}Xe relaxation in blood. As the contribution from deoxyhemoglobin is larger than that of oxygen in solution, the xenon spin-lattice relaxation time in deoxygenated blood is shorter than in oxygenated blood. For similar oxygenation level, the ^{129}Xe T_1 is longer at 37°C than at 25°C. The ratio of the relaxation times of oxygenated to deoxygenated blood is the same at both temperatures.

At a temperature of 37°C and at a magnetic field of 1.5 T, we measured a ^{129}Xe spin-lattice relaxation time of 6.4 s $\pm$ 0.5 s in arterial blood, and a T_1 of 4.0 s $\pm$ 0.4 s in venous blood. These values are comparable to typical blood transit times from the lungs to tissues such as the brain (27). Therefore, delivery of laser-polarized xenon to tissues is limited by loss of polarization during vascular transport. Intravenous injection of laser-polarized xenon in a suitable solution characterized by much longer ^{129}Xe T_1 and higher xenon solubility (13, 28, 29) might increase the hyperpolarized ^{129}Xe NMR signal from the target tissue. However, the difference of the xenon spin-lattice relaxation times in oxygenated and deoxygenated blood could be exploited as a potential contrast mechanism for hyperpolarized ^{129}Xe functional MRI.

By introducing flucloxacillin, we have demonstrated that xenon binding to albumin affects the xenon spin-lattice relaxation time in plasma. We believe that using competitive binding is a promising technique for studying the specificity of xenon-protein interactions, as we have demonstrated in our measurements in BSA solution. This method could be applied, for instance, to investigate the general anesthetic properties of xenon (21) and their origins in more detail.

We thank J. Iqbal and M. Booth for their help with sample characterization. Financial support from the Institute of Cancer Research and from the Cancer Research Campaign (CRC Grant SP/1780/0103) is gratefully acknowledged.

1. Happer, W., Miron, E., Schaefer, S., Schreiber, D., van Wijngaarden, W. A. & Zeng, X. (1984) *Phys. Rev. A* **29,** 3092–3110.
2. Walker, T. G. & Happer, W. (1997) *Rev. Mod. Phys.* **69,** 629–642.
3. Raftery, D., Long, H., Meersmann, T., Grandinetti, P. J., Reven, L. & Pines, A. (1991) *Phys. Rev. Lett.* **66,** 584–587.
4. Albert, M. S., Cates, G. D., Driehuys, B., Happer, W., Saam, B., Springer, C. S., Jr. & Wishnia, A. (1994) *Nature (London)* **370,** 199–201.
5. Wagshul, M. E., Button, T. M., Li, H. F., Liang, Z., Springer, C. S., Zhong, K. & Wishnia, A. (1996) *Magn. Reson. Med.* **36,** 183–191.
6. Miller, K. W., Reo, N. V., Schoot Uiterkamp, A. J. M., Stengle, D. P., Stengle, T. R. & Williamson, K. L. (1981) *Proc. Natl. Acad. Sci. USA* **78,** 4946–4949.
7. Swanson, S. D., Rosen, M. S., Agranoff, B. W., Coulter, K. P., Welsh, R. C. & Chupp, T. E. (1997) *Magn. Reson. Med.* **38,** 695–698.
8. Peled, S., Jolesz, F. A., Tseng, C.-H., Nascimben, L., Albert, M. S. & Walsworth, R. L. (1996) *Magn. Reson. Med.* **36,** 340–344.
9. Martin, C. C., Williams, R. F., Gao, J.-H., Nickerson, L. D. H., Xiong, J. & Fox, P. T. (1997) *J. Magn. Reson. Imaging* **7,** 848–854.
10. Mugler, J. P., III, Driehuys, B., Brookeman, J. R., Cates, G. D., Berr, S. S., Bryant, R. G., Daniel, T. M., de Lange, E. E., Downs, J. H., III, Erickson, C. J., *et al.* (1997) *Magn. Reson. Med.* **37,** 809–815.
11. Jameson, C. J., Jameson, A. K. & Hwang, J. K. (1988) *J. Chem. Phys.* **89,** 4074–4081.
12. Albert, M. S., Schepkin, V. D. & Budinger, T. F. (1995) *J. Comput. Assist. Tomogr.* **19,** 975–978.
13. Bifone, A., Song, Y.-Q., Seydoux, R., Taylor, R. E., Goodson, B. M., Pietrass, T., Budinger, T. F., Navon, G. & Pines, A. (1996) *Proc. Natl. Acad. Sci. USA* **93,** 12932–12936.

14. Albert, M. S., Balamore, D., Sakai, K., Kacher, D., Walsworth, R. L., Oteiza, E. & Jolesz, F. A. (1996) *International Society for Magnetic Resonance in Medicine (ISMRM) Fourth Meeting Proceedings* (ISMRM, Berkeley, CA), p. 1357.
15. Tseng, C. H., Peled, S., Nascimben, L., Oteiza, E., Walsworth, R. L. & Jolesz, F. A. (1997) *J. Magn. Reson.* **126,** 79–86.
16. Kacher, D. F., Balamore, D., Jolesz, F. A. & Albert, M. S. (1997) *International Society for Magnetic Resonance in Medicine (ISMRM) Fifth Meeting Proceedings* (ISMRM, Berkeley, CA), 1403.
17. Pauling, L. & Coryell, C. D. (1936) *Proc. Natl. Acad. Sci. USA* **22,** 159–163.
18. Tilton, R. F. & Kuntz, I. D. (1982) *Biochemistry* **21,** 6850–6857.
19. Zhao, L., Mulkern, R., Tseng, C.-H., Williamson, D., Patz, S., Kraft, R., Walsworth, R. L., Jolesz, F. A. & Albert, M. S. (1996) *J. Magn. Reson. B* **113,** 179–183.
20. Patyal, B. R., Gao, J.-H., Williams, R. F., Roby, J., Saam, B., Rockwell, B. A., Thomas, R. J., Stolarski, D. J. & Fox, P. T. (1997) *J. Magn. Reson.* **126,** 58–65.
21. Albert, M. S., Springer, C. S., Murphy, R. & Wishnia, A. (1992) *Proceedings of the Society of Magnetic Resonance in Medicine (SMRM) 11th Annual Meeting* (SMRM, Berkeley, CA), p. 2104.
22. Siggaard-Andersen, O., Wimberley, P. D., Gothgen, I. H. & Siggaard-Andersen, M. (1984) *Clin. Chem.* **30,** 1646–1651.
23. Siggaard-Andersen, O., Wimberley, P. D., Gothgen, I. H., Fogh-Andersen, N. & Rasmussen, J. P. (1988) *Scand. J. Clin. Lab. Invest.* **48,** 85–88.
24. Schoenborn, B. P. (1965) *Nature (London)* **208,** 760–762.
25. Tortora, G. J. & Anagnostakos, N. P. (1987) *Principles of Anatomy and Physiology* (Harper & Row, New York).
26. Jenkins, B. G. (1991) *Life Sci.* **48,** 1227–1240.
27. West, J. B. (1995) *Respiratory Physiology—The Essentials* (Williams & Wilkins, Baltimore).
28. Goodson, B. M., Song, Y.-Q., Taylor, R. E., Schepkin, V. D., Brennan, K. M., Chingas, G. C., Budinger, T. F., Navon, G. & Pines, A. (1997) *Proc. Natl. Acad. Sci. USA* **94,** 14725–14729.
29. Wolber, J., Rowland, I. J., Leach, M. O. & Bifone, A. (1999) *Magn. Reson. Med.*, in press.